

Some modeling requirements for wall models in large eddy simulation

By Jeffrey S. Baggett

1. Motivation and objectives

Large eddy simulation (LES) works when the energy-containing eddies of the flow are representable on the numerical grid. Unfortunately, in turbulent wall-bounded flows, outside the viscous sub-layer, these eddies can scale as the distance from the wall. As the Reynolds number increases and the viscous sub-layer shrinks, the number of grid points required to resolve the near-wall eddies increases dramatically. This near-wall resolution requirement is currently the severest bottleneck in applying LES to flows of practical interest (Chapman 1979, see also Baggett, Jiménez, and Kravchenko in this volume).

Deardorff (1970), in the first simulation of turbulent channel flow, was the first to use a wall model to avoid resolving the near-wall region in an LES. Computational resources were limited, 6720 grid points were the maximum number that would fit in core memory, and the first near-wall grid point had to be located well outside the viscous sub-layer, thus rendering the computed wall shear stresses highly inaccurate. To remedy this deficiency Deardorff constrained the wall-normal second derivatives of the horizontal velocities at the first off-wall grid point in such a way that the logarithmic law of the wall was satisfied in the mean. Effectively, an instantaneous logarithmic law was used to parameterize the wall shear stresses in terms of the horizontal velocities at the first off-wall grid point.

Since 1970, a number of other wall models have been proposed for use in LES of attached flows. Nearly all of them estimate the wall shear stresses which are used as boundary conditions for the core flow LES (along with zero wall-normal velocity at the wall). As of this writing, there are essentially three kinds of wall models that have been employed in LES.

The first and most widely used kind of wall model is an equilibrium stress model. The logarithmic law of the wall is applied locally to relate the horizontal velocities at some point above the wall to the wall shear stresses. As originally proposed by Schumann (1975), deviations from the mean wall shear stress are assumed to be linearly correlated to deviations from the mean horizontal velocities. This assumption yields an algebraic, possibly nonlinear, relation between the instantaneous wall shear stress and the off-wall horizontal velocity. A number of variations and improvements on this scheme have been proposed (see Piomelli, *et al.* 1989 for a review), but they are all based on an equilibrium stress assumption and their range is, therefore, limited.

A second kind of model, which has much in common with domain decomposition techniques, uses the three-dimensional boundary layer equations with a wall-damped eddy viscosity to represent the near wall region (Cabot 1995, Balaras *et*

al. 1996). The standard LES equations are solved on a coarse grid, with the first off-wall grid point located outside the buffer layer, using wall shear stress and zero transpiration boundary conditions. The wall shear stresses are provided by integrating the three-dimensional boundary layer equations on a grid embedded between the wall and the first off-wall LES grid point. The boundary conditions used for the boundary layer equations are no-slip at the wall, and the velocities are matched to the LES velocities at the first LES off-wall grid point. While the boundary layer equations are cheaper to solve numerically than the LES equations, this approach is still expensive since the grid required in the near-wall region for the boundary layer equations is similar to that required if the original LES were simply to resolve the near-wall region. Furthermore, this approach does not make sense in flows which do not exhibit boundary layers, e.g. separated flows. However, the general idea of applying a domain decomposition strategy and using different constitutive equations in near-wall domains may prove valuable for the general wall modeling problem.

The two kinds of wall models mentioned above apply to a limited class of flows; however, a third approach has been developed which, in principle, can be applied to develop wall models for arbitrary flows. In this approach linear stochastic estimation is used to find the best least squares estimate of the wall stresses given the LES velocities on some plane, or planes, parallel to the wall (Bagwell 1993, Bagwell 1994). Again, the estimated wall shear stresses are used as boundary conditions for the LES. Bagwell successfully employed the resulting wall model in LES of channel flow at $Re_\tau = 180$, but attempts to re-scale the wall model to apply it in an LES of channel flow at $Re_\tau = 640$ met with limited success. While this approach is a general mathematical approach and does not rely on the underlying physics, the two-point correlation tensor of the flow must be known to form the linear stochastic estimation coefficients.

None of the existing wall models seems to be a great candidate for use in LES of complex flows (see Cabot in this volume). Algebraic wall models based on equilibrium conditions are too simple to deal with complex flows, and solving three-dimensional boundary layer equations is expensive and also not easily extended to non-attached flows. One of the goals of the current study is to determine what information is needed from the near-wall region for accurate LES of the core flow. In other words, we would like to establish a target for the further development of wall models. Once a well-defined target is established, it will be the object of further studies to inquire as to whether or not simpler (than full Navier–Stokes or other three-dimensional PDE’s) systems, such as low-dimensional dynamical systems, are capable of producing the necessary near-wall information.

In this preliminary study we seek to answer the following question: What information does the core flow need from the near-wall region; that is, what does a wall model have to provide?

2. Accomplishments

To gain some insight into the questions asked above we have conducted some experiments using a coarse grid direct numerical simulation (DNS) of turbulent

channel flow. The DNS was performed using a second order finite difference code (Morinishi 1995). The grid is staggered and stretched in the wall-normal direction using a hyperbolic tangent mapping. Time is advanced using a three-stage Runge Kutta, fractional step scheme in which the wall-normal viscous terms are treated implicitly. The flow domain is 2π , $2\pi/3$, and 2 in the streamwise (x), spanwise (z), and wall-normal (y) directions, respectively. The domain is discretized by 32, 32, and 33 grid volumes in the streamwise, spanwise, and wall-normal directions. The Reynolds number, Re_τ , based on the channel half-width, h , and the friction velocity, u_τ , is 200. Unless otherwise noted, all simulations were performed with a constant pressure gradient in the streamwise direction.

Our experimental strategy will begin with a fully developed field as an initial condition and then do a simulation while saving the velocity and/or velocity gradient data on some parallel planes above the wall. The time series of boundary data, or modifications of the time series, is then used to provide boundary conditions to conduct simulations of the flow between the designated boundary plane and the far wall. By making selective modifications to the the time series of boundary data, we can gain insight into what information the near-wall flow must provide for accurate simulation of the core flow.

A possible objection to this study is that a simulation of turbulent channel flow at $Re_\tau = 200$ using only 32^3 grid points is hardly a DNS, and since we have not included an SGS model it is not properly an LES either. However, the resolution is similar to that employed in an LES, and the numerical scheme has enough artificial dissipation that the reference simulation gives remarkably good results. Our goal is simply to achieve the same core flow results with the modified boundary data simulations as in the reference simulation. An SGS model will have to be included in further studies, but for this preliminary study we chose to eliminate that possible source of uncertainty.

2.1 Choice of off-wall boundary conditions

There are many possible choices for supplying boundary conditions to the simulation at some height above the wall. Two possibilities are:

- (1) **Dirichlet:** velocities are specified where they are demanded on the staggered grid. In our case, we specify

$$u(x, y^+ \approx 25, z, t), v(x, y^+ \approx 30, z, t), w(x, y^+ \approx 25, z, t),$$

from the reference time series. This fixes the transpiration velocity at the computational boundary and also guarantees the right correlations between u and v at the computational boundary. Note that this does not fix the value of $\langle u'v' \rangle$ at the computational boundary since that is determined by interpolating values of u and v on the staggered grid, and only half of those interpolated values of u are fixed by the boundary condition.

- (2) **Mixed:** transpiration velocity and wall-normal gradients of the horizontal velocities are specified on the plane $y^+ \approx 30$:

$$\frac{\partial u}{\partial y}(x, y^+ \approx 30, z, t), v(x, y^+ \approx 30, z, t), \frac{\partial w}{\partial y}(x, y^+ \approx 30, z, t).$$

This fixes the viscous stresses and the transpiration velocity at the plane $y^+ \approx 30$.

Morinishi's DNS code was modified to take either form of boundary condition, and a reference time series of 12,000 time steps, corresponding to $60h/u_\tau$ time units, of boundary data was saved by integrating a fully developed field. As in all the subsequent simulations, the boundary data time series was used to provide boundary conditions for a simulation with one wall removed from the computation. All of the simulations with off-wall boundary data are integrated for the length of the time series, $60h/u_\tau$, with statistics collected over the last $30h/u_\tau$ time units.

First, to test the application of the two types of off-wall boundary conditions, simulations were conducted using the same initial condition as used to generate the time series. The simulation employing the Dirichlet off-wall boundary conditions produced mean flow and second order statistics which were indistinguishable from the reference simulation. This is hardly surprising since no changes were made to the numerical scheme to accommodate the Dirichlet boundary conditions. Any differences in the simulated flow with off-wall boundary conditions and the reference simulations, when using the same initial condition, should be due to round-off errors.

The mixed off-wall boundary conditions did not work as well. The wall-normal gradients of the horizontal velocities are fixed at the computational boundary, $y^+ \approx 30$, but the horizontal velocities themselves are not fixed. Eventually the streamwise velocity, u , "slips" and is no longer correlated properly with the wall-normal velocity, v , which is fixed by the time series. This leads to an under-prediction of the turbulent stresses near the computational boundary, which in turn causes the mean flow to accelerate. Shown in Fig. 1 are statistics accumulated over the last $30h/u_\tau$ time units of a simulation with mixed off-wall boundary conditions conducted over the length of the time series, $60h/u_\tau$ time units. Bagwell (1994) had similar difficulties in attempting to use a wall model to provide the same off-wall mixed boundary conditions in turbulent channel flow.

The Dirichlet off-wall boundary conditions appear to work better. To test their robustness, another simulation was performed with the same time series, but using an initial field completely different than the one used to generate the time series. Initially, the boundary data and the start field are incompatible, and this leads to an under-prediction of the turbulent stresses near the computational boundary. In the absence of enough opposing force, due to the constant pressure gradient, the flow accelerates initially and then slowly, over viscous time scales, settles to the expected mean flow. To accelerate convergence of the statistics, a pressure gradient control scheme was used in the initial $30h/u_\tau$ time units to drive the flow towards one with the expected mass flux. This control scheme was then turned off, and the statistics, shown in Fig. 2, are accumulated over the last $30h/u_\tau$ time units. There are some small discrepancies in the second order statistics which may be statistical.

The fact that the simulation, with Dirichlet off-wall boundary conditions and an inconsistent start field, converges at all suggests that the core flow is responding passively to events in the near-wall region. Perhaps this is not surprising since the main region of turbulent production occurs below the point where the off-wall boundary condition is supplied to the flow. The core flow may be able to be

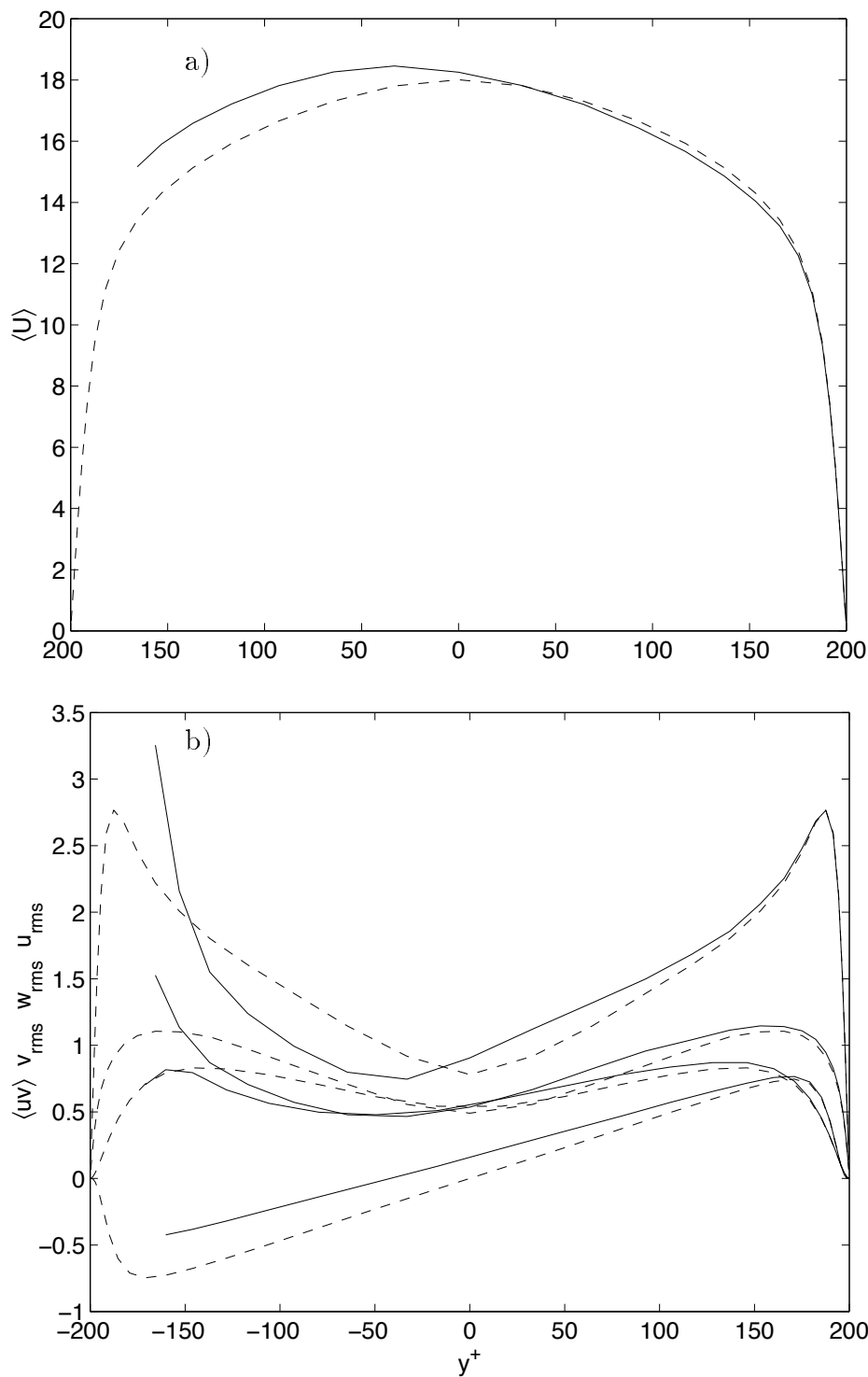


FIGURE 1. Mixed off-wall boundary conditions. Dashed lines show the statistics from the reference simulation used to generate the time series. Solid lines show the statistics from the simulation with mixed off-wall boundary conditions provided at $y^+ \approx 30$ from the time series. Plot a) shows the mean flow, and plot b) shows the r.m.s. velocities and the Reynolds shear stress. The four sets of curves, from top to bottom on the left hand side, correspond, in order, to u_{rms} , w_{rms} , v_{rms} , and $\langle u'v' \rangle$.

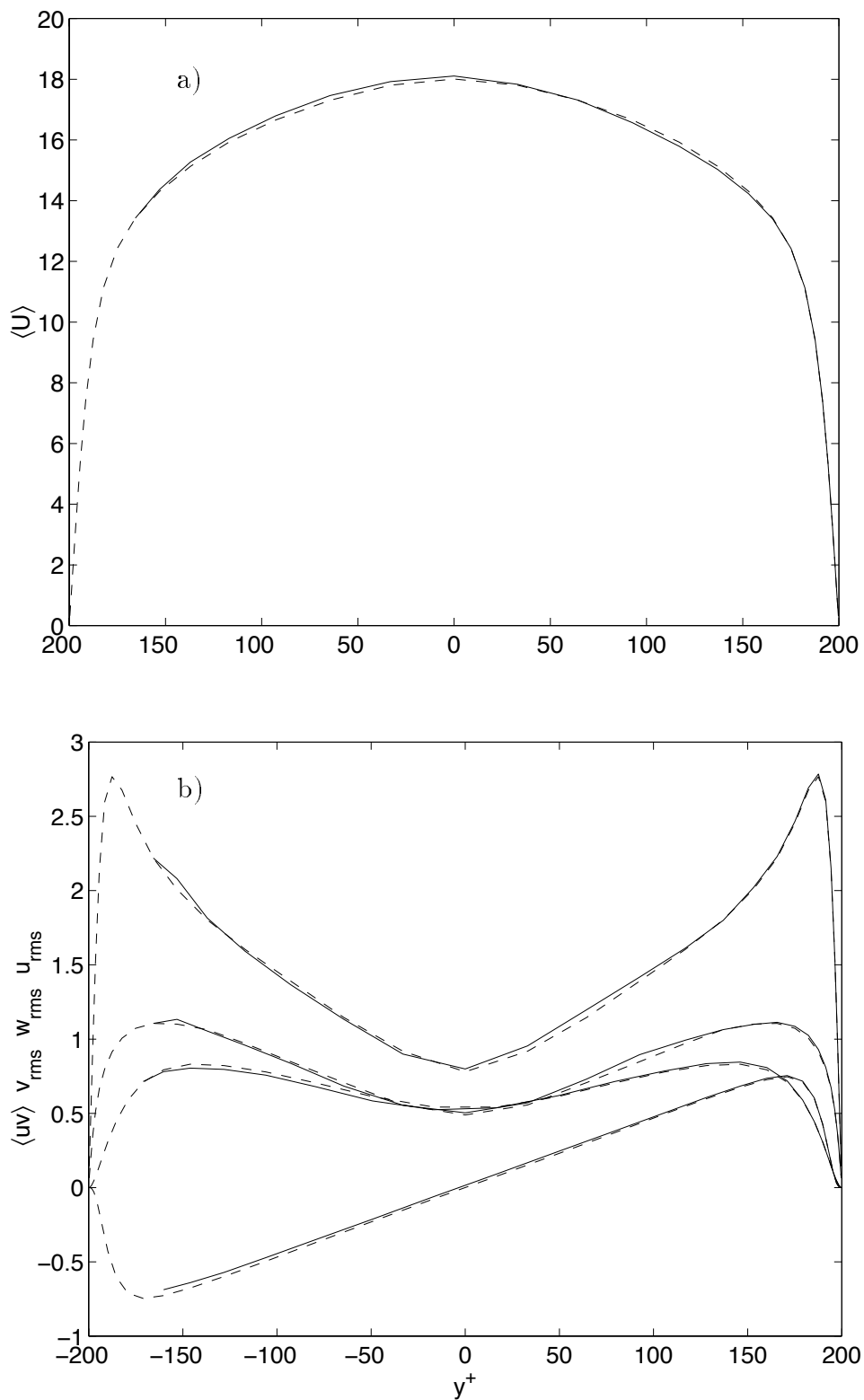


FIGURE 2. Dirichlet off-wall boundary conditions with inconsistent start field. As in Fig. 1 the dashed and solid lines show the reference and off-wall boundary condition simulations, respectively. Plots a) and b) show the same quantities as in Fig. 1.

simulated by providing a time series of good turbulence data on some plane between the core flow and the region of turbulence production, but it remains to be seen if this boundary data can be provided by a cheap wall model. In any case, the Dirichlet off-wall boundary condition is extremely robust, and we will use it below to study the information flux from near-wall region to the core flow.

2.2 Mildly scrambled Dirichlet data

Providing a good time series of velocity boundary data to the core flow is sufficient to conduct an accurate simulation of just the core flow region. To begin to understand just what structural information has to be incorporated into the velocity boundary data, we make various modifications to the boundary data in this section and the next.

One particularly gentle way to perturb the structure of the boundary data is to randomize the phases of the Fourier components. If the same random phase angle is applied to all three velocity components for each wavenumber vector, then the horizontal spectra and cospectra are not perturbed. The transformation is

$$(\hat{u}_j^s(y), \hat{v}_j^s(y), \hat{w}_j^s(y)) = e^{i\theta_j} (\hat{u}_j(y), \hat{v}_j(y), \hat{w}_j(y)),$$

where \hat{u} and \hat{u}^s denote the Fourier coefficients of the original and scrambled data, respectively. θ_j is a random phase angle chosen uniformly from the interval $[-\pi, \pi)$. Since the boundary data is real, the relation $\theta_j = -\theta_{-j}$ must be satisfied. This transformation has the further advantage that the continuity relation is not affected:

$$k_x \hat{u}_j^s(y) + \frac{\partial}{\partial y} \hat{v}_j^s(y) + k_z \hat{w}_j^s(y) = 0.$$

Thus the horizontal spectra of $\partial v / \partial y$ are not effected at the computational boundary, that is, the mass flux through the boundary plane maintains much of its original structure. Furthermore, the random phase angles are constant with respect to time, so the boundary data maintains its original time scales. Even though the original structure of the Dirichlet boundary is lost, in particular all of the moments of order greater than two are perturbed, the core flow is still simulated well (see Fig. 3).

This result suggests that the core flow can be simulated without complete structural information from the near-wall region. However, as we shall see in the next section, some structural information is necessary.

2.3 Severely scrambled Dirichlet data

We have just shown that the core flow simulation can tolerate some loss of structural information from the near-wall region. Here, we will check to see if it is sufficient to supply boundary data information which has the correct second order statistics and time scales, but for which the turbulence structure is severely perturbed.

One way to achieve such an effect is to randomize the phases of the Fourier components, but, as opposed to the method applied in the previous section, the

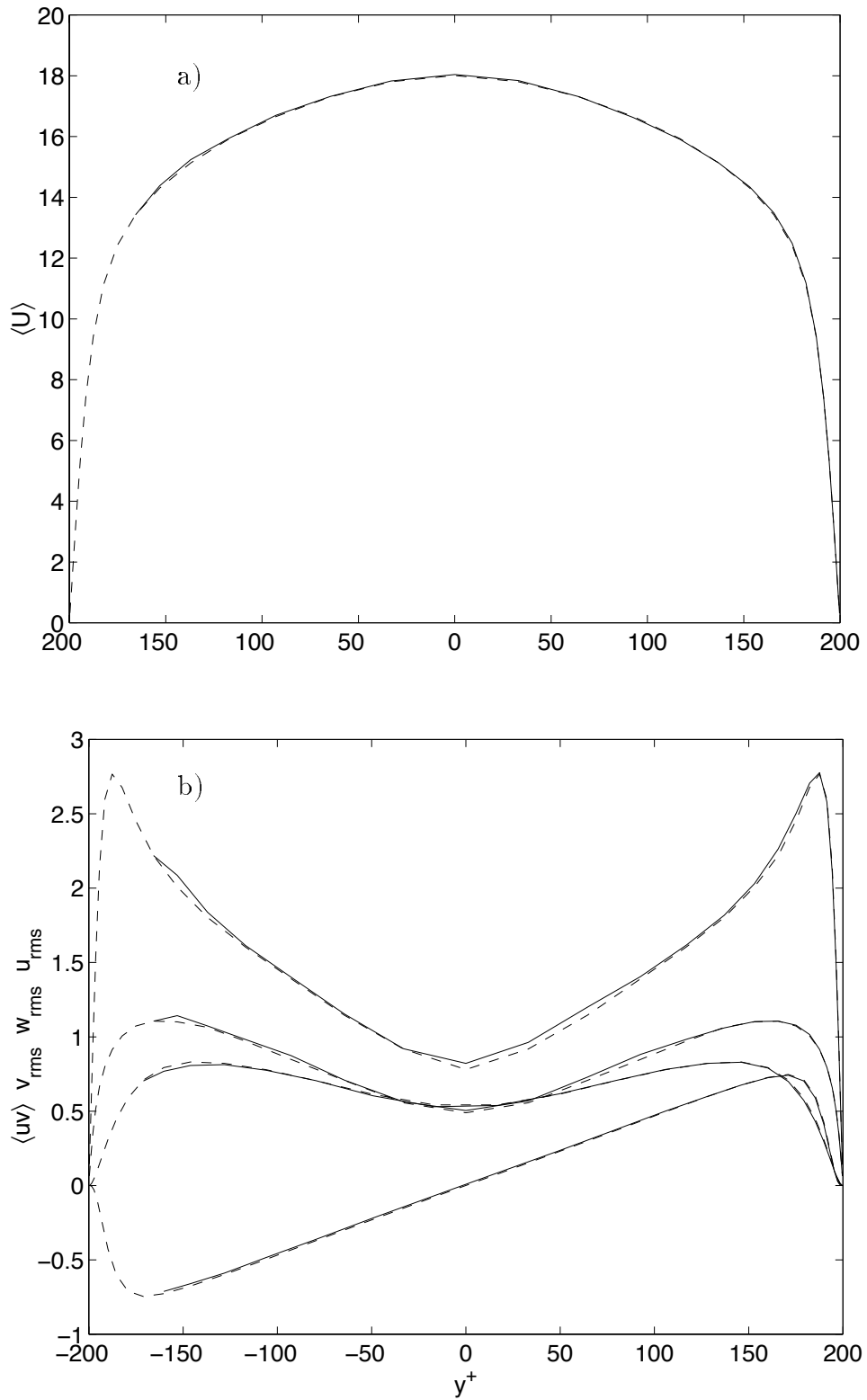


FIGURE 3. Mildly scrambled off-wall Dirichlet boundary conditions. As in Fig. 1 the dashed and solid lines show the reference and off-wall boundary condition simulations, respectively. Plots a) and b) show the same quantities as in Fig. 1.

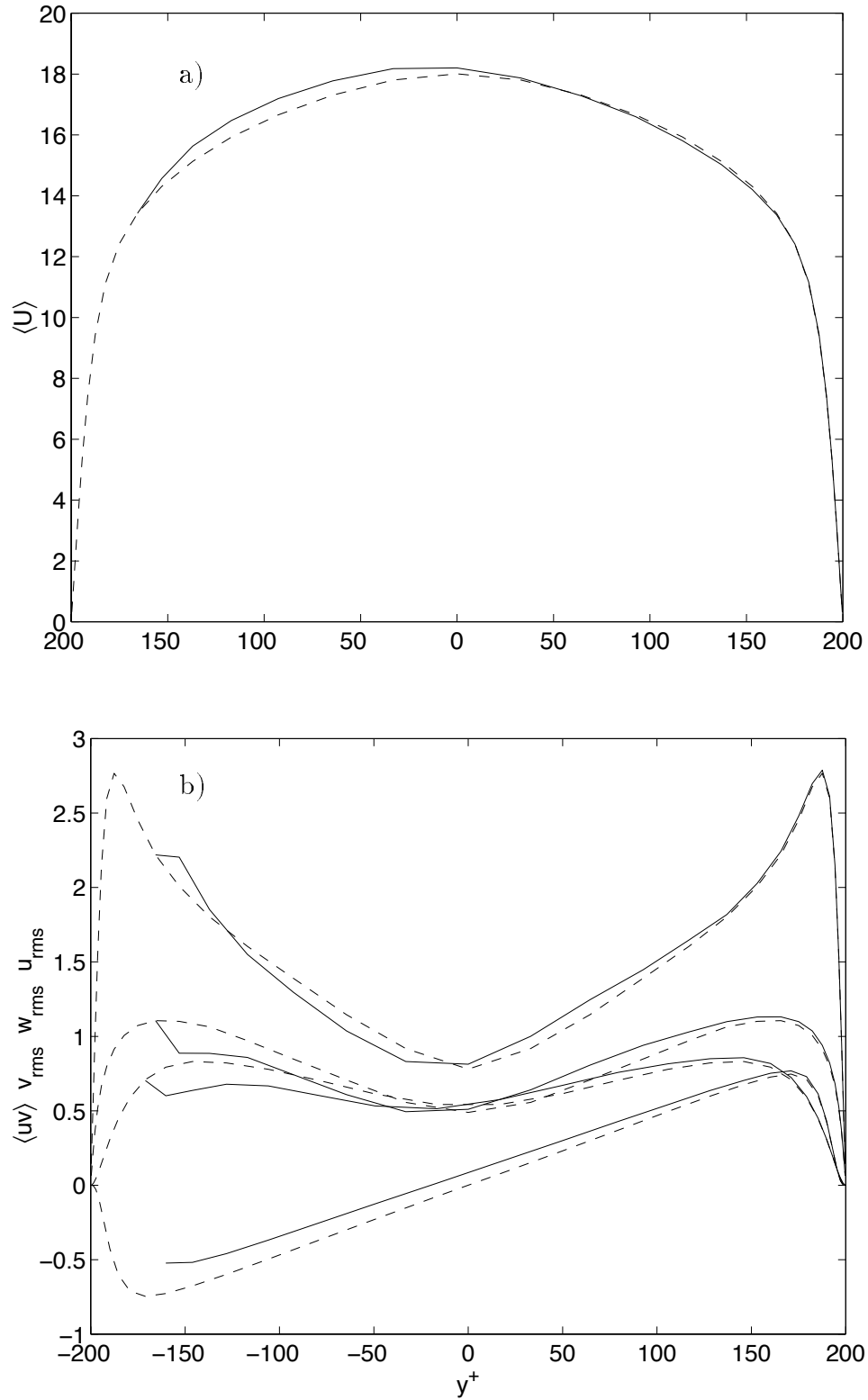


FIGURE 4. Severely scrambled off-wall Dirichlet boundary conditions. As in Fig. 1 the dashed and solid lines show the reference and off-wall boundary condition simulations, respectively. Plots a) and b) show the same quantities as in Fig. 1.

random phase angle is chosen independently for each of the velocity components for each wavenumber vector. That is,

$$(\hat{u}_j^r(y), \hat{v}_j^r(y), \hat{w}_j^r(y)) = (e^{i\theta_j^1} \hat{u}_j(y), e^{i\theta_j^2} \hat{v}_j(y), e^{i\theta_j^3} \hat{w}_j(y)).$$

The Fourier coefficients \hat{u}_j are those of the original boundary data, and \hat{u}_j^r are the those of an intermediate set of boundary data. The phase angles $\theta_j^i, i = 1, 2, 3$ are chosen uniformly and independently from the interval $[-\pi, \pi)$, and $\theta_j^i = -\theta_{-j}^i$ so that the boundary data remains real. The relative phase angles between the Fourier coefficients for the u^r and v^r boundary data are changed by this transformation so that $\langle(u^r - \langle u^r \rangle)v^r\rangle$ is also changed. But, by following the technique used by Lee *et al.* (1992) to generate random inflow data for a turbulent simulation, we can rotate the principal axes of u^r and v^r to obtain the correct correlation for the scrambled boundary data. Finally, the scrambled boundary data are given by:

$$u^s = \cos(\psi)u^r + \sin(\psi)v^r,$$

$$v^s = -\sin(\psi)u^r + \cos(\psi)v^r,$$

and

$$w^s = w^r.$$

Details on solving for the rotation angle ψ are given in (Lee *et al.* 1992).

The scrambled boundary data have the correct mean values and second order statistics, but the spectra and cospectra are perturbed. Furthermore the structure of $\partial v / \partial y$ is strongly perturbed through the continuity relation mentioned in the previous section. The random phase angles are constant with respect to time, so the scrambled boundary data still has the correct time scales, but the boundary data are effectively random numbers with the correct second order statistics. w^s has the same horizontal spectra as the original boundary data, but the spectra of u^s and v^s are modified by rotation of their principal axes as are the cospectra.

Again, the simulation was run over $60h/u_\tau$ time units with statistics accumulated over the last $30h/u_\tau$ time units. As can be seen in Fig. 4, the mean flow and second order statistics develop a boundary layer type character near the computational boundary. This indicates that simply providing a time series of boundary data with the correct second order statistics, approximately the correct spectra, and the correct time scales is insufficient for the accurate simulation of the core flow.

3. Conclusions

Off-wall boundary conditions can be used for simulation of just the core region of a turbulent channel flow. Our results indicate that supplying velocity boundary data may be more robust than attempting to fix the wall-normal gradients of the horizontal velocities as well as the transpiration velocity through the computational boundary plane. This may not be surprising since outside of the near-wall viscous sub-layer the total stress is dominated by the contribution from the turbulent stresses. The off-wall Dirichlet boundary conditions fix the correlation between

u and v at the boundary, whereas the mixed off-wall boundary conditions fix only the viscous stresses at the computational boundary.

These preliminary results also suggest that the off-wall velocity boundary conditions must contain at least some turbulence structure. In particular, the simulations performed with the “mildly” scrambled velocity boundary conditions suggests that boundary data with the correct spectra and cospectra may be sufficient for accurate simulation of the core flow. Correct estimation of moments greater than second order is probably not necessary. However, simply supplying the correct statistics, up to second order, is not sufficient — some further structural information is necessary. Thus, even if the second order statistics of the near-wall region are known, it may be difficult to use this information to extrapolate boundary conditions from the core flow as suggested by Carati (in this volume).

On a final note, to see what may happen if structural information about the near-wall region is not incorporated into the wall model, consider the large-eddy simulations of Mason and Callen (1986). They attempted to simulate high Reynolds number turbulent channel flow by forcing the flow to fit a local logarithmic law at the wall along with zero wall-normal transpiration. Their boundary condition guarantees the right total stress in the mean but is incapable of carrying the right turbulence structure. Effectively, they completely excised the region of turbulence production from their computation and used a wall model without any capacity to correct this deficiency. They found that they were unable to simulate an effective logarithmic region in their calculations. This problem was later rectified by Mason and Thomson (1992) by including a stochastic backscatter term which probably helped compensate for the missing production mechanism. It is clear that the core flow needs to see at least some of the turbulence structure produced in the near-wall region. It remains to be seen if cheap wall models can provide the necessary turbulence structure to the core flow.

REFERENCES

- BAGWELL, T. G., ADRIAN, R. J., MOSER, R. D. & KIM, J. 1993 Improved approximation of wall shear stress boundary conditions for large eddy simulation, in *Near-Wall Turbulent Flows*, eds. R. M. C. So, C. B. Speziale, & B. E. Launder (Elsevier Science Publishers).
- BAGWELL, T. G. 1994 Stochastic Estimation of near wall closure in turbulence models, Ph.D. thesis, Univ. Illinois Urbana-Champaign.
- BALARAS, E., BENOCCI, C. & PIOMELLI, U. Two-layer approximate boundary conditions for large-eddy simulations *AIAA J.* **34**, 1111-1119.
- CABOT, W. 1995 Large-eddy simulations with wall models. *CTR Research Briefs* Center for Turbulence Research, NASA Ames/Stanford Univ., 41-50.
- CHAPMAN, D. R. 1979 Computational aerodynamics development and outlook. *AIAA J.* **17**, 1293-1313.
- DEARDORFF, J. W. 1970 A numerical study of three-dimensional turbulent channel flow. *J. Fluid Mech.* **41**, 453-480.

- LEE, S., LELE, S. K. & MOIN, P. 1992 Simulation of spatially evolving turbulence and the applicability of Taylor's hypothesis in compressible flow. *Phys. Fluids A*, **4**, 1521-1530.
- MASON, P. J. & CALLEN, N. S. 1986 On the magnitude of the subgrid-scale eddy coefficient in large-eddy simulations of turbulent channel flow. *J. Fluid Mech.* **162**, 439-462.
- MASON, P. J. & THOMSON, D. J. 1992 Stochastic backscatter in large-eddy simulations of boundary layers. *J. Fluid Mech.* **242**, 51-78.
- MORINISHI, Y. 1995 Conservative properties of finite difference schemes for incompressible flow. *CTR Research Briefs* Center for Turbulence Research, NASA Ames/Stanford Univ., 121-132.
- PIOMELLI, U., FERZIGER, J., MOIN, P. & KIM, J. 1989 New approximate boundary conditions for large eddy simulations of wall-bounded flows. *Phys. Fluids*, **1**, 1061-1068.
- SCHUMANN, U. 1975 Subgrid scale model for finite difference simulations of turbulent flows in plane channels and annuli. *J. Comp. Phys.* **18**, 376-404.